Applied Catalysis B: Environmental 86 (2009) 1–7

Contents lists available at ScienceDirect

Applied Catalysis B: Environmental

journal homepage: www.elsevier.com/locate/apcatb

Review

Synthesis and photocatalytic properties of dense and porous TiO_2-anatase thin films prepared by sol–gel

N. Arconada [a], A. Durán [a], S. Suárez [b], R. Portela [b], J.M. Coronado [b], B. Sánchez [b], Y. Castro [a,*]

[a] Instituto de Cerámica y Vidrio (CSIC), Campus de Cantoblanco, Kelsen 5, Cantoblanco, 28049 Madrid, Spain
[b] CIEMAT-PSA, Avda Complutense 22, 28040 Madrid, Spain

ARTICLE INFO

Article history:
Received 17 April 2008
Received in revised form 17 July 2008
Accepted 24 July 2008
Available online 31 July 2008

Keywords:
Sol–gel TiO_2 coatings
Template (PEG)
Photocatalysis
Trichloroethylene

ABSTRACT

Porous TiO_2-anatase films were prepared by sol–gel route showing higher photocatalytic activity in degradation of trichloroethylene (TCE) in air compared to dense titania films. Titania sols were synthesized with and without a pore generating agent, polyethylene glycol (PEG), to evaluate the effect of porosity in the photocatalytic activity of the coatings. The films were deposited by dipping and sintered at different temperature and time. The characterisation was performed by profilometry, Fourier transform infrared spectroscopy (FTIR), grazing X-ray diffraction (GXRD) and field emision scan electron microscopy (FE-SEM), observing that anatase phase is obtained at temperatures as low as 350 °C. The maximum specific surface area (S_s = 43 m^2/g) was obtained for coatings prepared from TiO_2 sol with PEG and sintered at 400 °C. Porous TiO_2-anatase films present TCE conversion around 20% higher than that of dense films. Porous volume, surface area and thickness of the coating play a key role in the photocatalytic activity. On the other side, variation in particle size seems not to be a critical parameter in the studied range.

Contents

1. Introduction

Volatile organic compounds (VOCs) are recognized as dangerous pollutant compounds. Besides being carcinogen agents and contribute to ozone production in the troposphere

* Corresponding author. Tel.: +34 91 7355840; fax: +34 91 7355843.
E-mail address: castro@icv.csic.es (Y. Castro).

0926-3373/$ – see front matter © 2008 Elsevier B.V. All rights reserved.
doi:10.1016/j.apcatb.2008.07.021

[1,2], the major problem arises from their high resistance to physical, chemical or biological treatments. The paint and adhesive industry, as well as combustion processes are among the most important anthropogenic sources of VOCs emissions into the atmosphere [3].

Photocatalysis is an efficient, attractive and clean technology for pollutant abatement either in aqueous media or in gas phase [4,5]. TiO_2 is the archetypical photocatalytic material since it is endowed with an inherent photocatalytic activity [6,7]. Moreover, it is inexpensive, very stable and available in large amounts. Specially for air treatment the usage of TiO_2 particles is not feasible due to the high costs of the concomitant filtration facilities needed to recover the catalyst and the risk to release TiO_2 particles into the atmosphere. Therefore, processes focused on the development of supported catalysts with high photocatalytic performance are receiving great attention in the last years either in air [8,9] or water treatments [10–12].

Different methods have been used to prepare TiO_2 films: reactive method [13], chemical vapour deposition, sputtering, pulsed laser deposition (PLD) [14] or hydrothermal method [15]. But sol–gel process is considered as one of the most promising alternatives because it presents a number of advantages such as low sintering temperature, versatility of processing and homogeneity at molecular level. This method allows obtaining TiO_2-anatase at low temperature. This phase has been extensively investigated because its high activity in photocatalytic applications [16,17].

TiO_2 powders and gels with porous structure and high photocatalytic performance have been reported [18,19]. However, the preparation of porous TiO_2 films with high specific surface area is attracting more and more attention [20–22]. Photocatalytic processes are chemical reactions on the surface. Thus, the increase of surface area should improve the efficiency of the process because it implicates larger contact surfaces exposed to the pollutants [23,24].

Porous inorganic TiO_2-anatase films can be obtained using templating membranes [25] or conventional alkoxide sol–gel route with the addition of surfactants [26]. The templates permit to retain the initial polymer morphology up to final porous structure. Polyethylene glycol is especially suitable for modifying the porous structure of coatings [27,28] due to its complete decomposition at relatively low temperature [29,30]. However, the control of synthesis and deposition processes is crucial for obtaining thick, crack-free and homogeneous coatings.

Crystalline phase, specific surface area, surface OH groups, morphology and aggregation of particles are some of the parameters playing a decisive role in the photocatalytic efficiency of titania [31,32]. However, diverse results can be found in literature. While some authors highlight the high surface area as determining factor to increase efficiency [33–35] others point out the influence of crystallinity and particle size [36].

The aim of this work was to investigate the photocatalytic activity of porous TiO_2-anatase coatings as a function of surface area, porosity, crystallinity and particle size using trichloroethylene (TCE) as VOC molecule. This compound has been widely used as a model pollutant in semiconductor photocatalysis because it can be easily photodegraded.

Porous coatings were prepared using a simple and easy to scale-up alkoxide route by adding polyethylene glycol (PEG) as pore generating agent. Dense nanocrystalline TiO_2-anatase thin films used as reference were also synthesized. The synthesis and heat treatment conditions were optimised for obtaining coatings with high crystallinity and surface area. An innovative method to determine surface area of coatings is also described.

2. Experimental

2.1. Synthesis and characterisation of sols

2.1.1. Synthesis of sols

Two titania sols (sol A and sol B) were prepared using titanium isopropoxide (TISP) as precursor via acid catalysis with the following route. First, TISP was chemically modified by adding acetyl-acetone (AcAc) to control the hydrolysis and condensation reactions. This solution was maintained for 1 h under stirring up to obtain the complex chelate. Ethanol mixed with acidified water (0.1N HCl) was added drop by drop to this solution to start hydrolysis and condensation reactions. The final molar ratio of sol A was 1 TISP:1 AcAc:40 EtOH:1 H_2O, the oxide concentration being fixed to 30 g/L. Sol A was aged for 1 day before coating deposition.

A similar process was used to prepare titania sol B but adding PEG (average molecular weight of 400) to the ethanol–acidified water. Different PEG amounts (1, 3, 5 and 10 mol%), were incorporated maintaining the previous molar ratios of precursors. Sol B was heated up to 80 °C for 1 h to ensure the reactivity between titania oligomers and PEG [21].

2.1.2. Viscosity

The stability of the sols was studied through the evolution of viscosity with time, using a rheometer (Haake, RS50, Germany) under controlled rate conditions. The shear rate was increased from 0 to 1000 s^{-1} in 5 min, with 1 min at the maximum rate and decreasing again to 0 in 5 min, at 25 °C.

2.2. Deposition and characterisation of coatings

2.2.1. Coatings deposition

A first layer of dense SiO_2 [37] (200 nm) was deposited onto the glass substrates to avoid the degradation of the photocatalytic activity [38]. This coating, with a 95% of theoretical density, has demonstrated to inhibit the diffusion of Na^+ cations from the glass substrate during firing [39,40].

TiO_2 films were deposited by dip-coating from TiO_2 sol A and TiO_2 sol B onto SiO_2 coated glass-slides and silicon wafers. The withdrawal rate varied from 5 to 60 cm/min. The coatings were treated in air at 350, 400, 450 and 500 °C for 1, 3 and 10 h using heating and cooling rates of 10 °C/min. Finally, multilayer coatings of each sol were prepared using an intermediate treatment of 200 °C/30 min between depositions.

2.2.2. Optical and field-emission scanning electron microscopy (FE-SEM) characterisation

Optical and FE-SEM (Hitachi-S4700, Japan) were used to study the homogeneity and microstructure of the coatings.

2.2.3. Fourier transform infrared spectroscopy (FTIR) and grazing X-ray diffraction (GXRD) characterisation

Coatings deposited onto silicon wafers were analysed by FTIR to study the structural evolution. FTIR spectra were recorded in transmission mode in the frequency range 4000–400 cm^{-1} with a resolution of 2 cm^{-1} using a PerkinElmer FTIR (Spectrum 100 equipment). The crystallisation of TiO_2-anatase was followed by grazing angle X-ray diffraction using CuKα radiation in a Bruker diffractometer (Siemens-D5000). The diffractrogram was recorded in 2θ ranges of 20–70° and 23–27°, using a fixed counting time of 20 s/step and 2θ increment of 0.03°. The crystallite size (D) of the coatings sintered at 350, 400, 450 and 500 °C for 1, 3 and 10 h was estimated using the Scherrer's

equation:

$$D = \frac{0.9\lambda}{\beta \cos\theta_B} \quad (1)$$

where λ is the wavelength of Kα (0.15409 nm), β the quartz standard-corrected full width at half-maximum (FWHM) of the Bragg peak (rad) and θ_B is the Bragg angle (°). The peak $2\theta_B = 25.2°$ was chosen as the main peak for determining anatase phase. The crystal fraction evolution was followed through the area of this peak.

2.2.4. Specific surface area

The specific surface area was analysed as a function of temperature and time following a method described by Durán and Nieto [41]. Glass-microspheres with size between 40 and 70 μm were placed in a glass column closed by a filter. Sol A and sol B were dripped through the microspheres in the column and shaken in order to homogenize the system. Then, a flow of N_2 was passed through the column to dry the product. The coated microspheres were separated in four parts and heat-treated at 350, 400, 450 and 500 °C for 1, 3 and 10 h. The amount of TiO_2 deposited onto the microspheres was determined by chemical analysis (XRF, MagiX PW2424, Philip, Holland) and the surface area was measured by N_2-adsorption BET method using a Monosorb Surface Area Analyser MS-13 (Quantachrome Co., USA). The surface area of the coatings was obtained through the equation:

$$\delta_{TiO_2} = \frac{\delta_{measured} - \delta_{microspheres}}{TiO_2 \text{ amount}} \quad (2)$$

where δ_{TiO_2} (m^2/g) is the surface are of TiO_2 coating, $\delta_{measured}$ (m^2/g) the value obtained through BET method with the coated microspheres, $\delta_{microspheres}$ (m^2/g) the surface area of the uncoated microspheres and TiO_2 amount, is the weight of TiO_2 obtained from chemical analysis.

2.2.5. Photocatalytic activity

The photocatalytic properties of the supported photo-catalysers were evaluated by studying the photocatalyst oxidation of TCE as a model VOCs molecule in a continuous plug flow gas-phase flat photoreactor. This photoreactor, with external dimensions 120 mm × 50 mm × 10 mm (length × wide × depth) was constructed in stainless steel except one window of 27 cm^2, closed with borosilicate glass with low iron content. Illumination is provided by two UVA Philips TL-8W/05 fluorescent lamps with a maximum emission at 365 nm wavelength and light intensity of 4.4 mW/cm^2. A gas mixture of TCE/ air was prepared using a gas cylinder of TCE/N_2 (Air Liquide, 500 ppm) and compressed air free of water and CO_2. The flow rate was controlled by using electronic mass flow controllers. The TCE concentration was maintained at 90 ppm, and the total gas flow was varied from 50 to 200 ml min^{-1} operating at residence time between 3.0 and 0.8 s. The TCE evolution with reaction time was analysed by gas chromatography using a Hewlett Packard HP6890 series with a flame injector detector (FID).

3. Results and discussion

3.1. TiO_2 sols and films

Homogeneous and transparent sols were obtained for both compositions. Viscosity of TiO_2 sol A and B with 1, 3, 5 and 10 mol% of PEG was measured at 25 °C. In all the cases, a Newtonian behaviour was observed with viscosities between 1.7 and 2 mPa s revealing a good stability for more than 1 month.

TiO_2 films were deposited by dip-coating from sol A and sol B using different withdrawal rates and heat treated at different temperatures and times. The coatings obtained from sol A present good optical quality being homogeneous, transparent and crack free, with a critical thickness of 80 nm after treated at 500 °C/1 h. In the case of sol B, the coatings obtained with 5 and 10 mol% of PEG presented some defects and roughness, making difficult the thickness measurement. A molar ratio of 3% was thus selected as the maximum amount of PEG compatible with homogeneous coatings. Under this condition, critical thickness of coatings with 3% molar of PEG was found near of 100 nm after treatment at 500 °C/1 h. This indicates that the addition of the surfactant generates thicker coatings compared to dense film, a phenomenon recently explained in porous coatings as the result of stress relaxation in pores [42].

3.2. Effect of sintering temperature and time in the crystallisation of TiO_2-anatase

The coatings prepared on silicon wafers from both sols were analysed by FTIR and GXRD to follow the crystallisation of TiO_2-anatase. FTIR spectra confirm that the coatings are free of organic residues. Fig. 1 shows the FTIR spectra of (a) TiO_2-sol A and (b) TiO_2-sol B coatings treated at 350 °C for different times. The band at 435 cm^{-1} assigned to TiO_2 in anatase phase [43] is clearly observed. For coatings obtained from sol A the band is only detected for the longest treatment of 10 h at 350 °C. However,

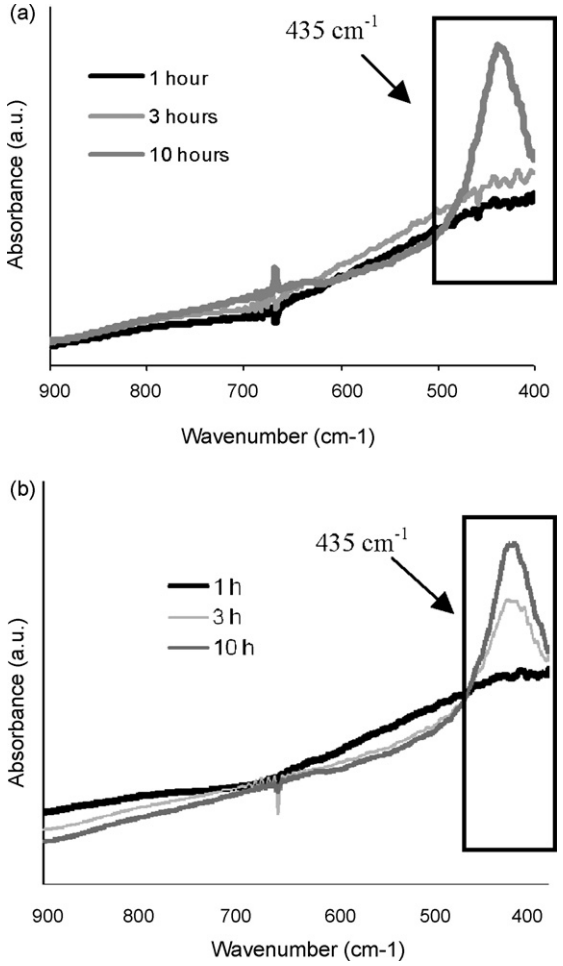

Fig. 1. FTIR spectra of (a) TiO_2-sol A and (b) TiO_2-sol B treated at 350 °C for different times.

coatings from sol B show this band after only 3 h of thermal treatment at the same temperature, showing that the incorporation of PEG permits to reduce the sintering time. For higher temperatures, anatase band appears clearly after 1 h of treatment. Thus, FTIR appears as a suitable and rapid method with high sensitivity to detect small amounts of anatase, though it is not strictly quantitative.

GXRD was further used to quantify the crystal size and area of peak (25.2°) as a function of temperature and sintering time. The area was calculated to evaluate the development of crystal fraction which is proportional to the area of the peak. The diffraction patterns of coatings of TiO_2 sol A and sol B with 3% PEG treated at different temperatures and times were obtained in the 2θ range of 20–70° (not shown). The main band at $2\theta \sim 25.2°$, associated to the (1 0 1) lattice plane of the tetragonal TiO_2-anatase phase (JCPDS-89-4921) was identified in both types of coatings. A narrower interval of 2θ (23–27°) was further used to follow the evolution of the width and area of the anatase peak as a function of temperature and time of heat treatment. Fig. 2 shows the GXRD spectra in this range for coatings from sol B treated at 500 °C for 1, 3 and 10 h. The peak corresponding to anatase increases slowly and becomes narrower and more symmetric with the sintering time, indicating a better crystallisation and/or higher crystal fraction. Even using severe heat treatment conditions, i.e. 500 °C/10 h TiO_2-rutile phase was not observed.

Fig. 3 shows the evolution of crystalline fraction, considered proportional to the area of (1 0 1) peak obtained from GXRD, as a function of temperature and time of the heat treatment. An important increment is observed for short treatments, associated with the rapid formation and/or growing of anatase crystals. Above 3 h of heat treatment, the crystalline fraction maintains quite constant for $T \geq 400$ °C. Coatings treated at 350 °C need a longer time (10 h) for total crystallisation.

The evolution of anatase crystal size (D) was estimated using the Scherrer's equation. The FWHM values were extracted from the XRD patterns fitted using the Peakfit software. The thickness and the calculated particle size of the coatings are represented in Fig. 4 as a function of temperature and sintering time. The coating thickness decreases with temperature and time of the thermal treatment due to contraction of the network associated with the sintering process. On the other hand, and in spite of the error is quite high (around 5%), an increasing trend in crystallite size with sintering temperature and time is apparent for 450 and 500 °C. At 400 °C the growing is much slower not being appreciable in the used time range. This behaviour is probably related with the activation energy necessary for an atom to leave the matrix and attach to the crystal that strongly depends on temperature [44]. A similar effect was observed in dense coatings obtained from sol A.

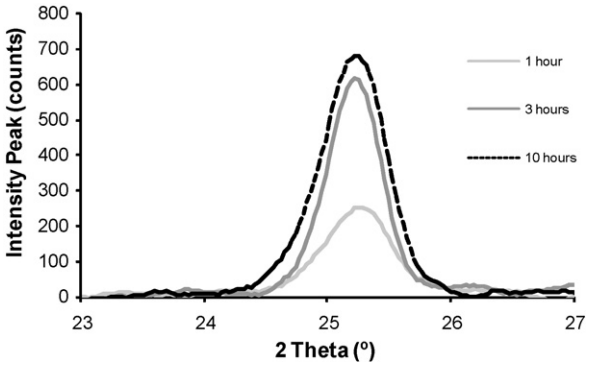

Fig. 2. GXRD spectra of coatings from TiO_2-sol B treated at 500 °C for different times.

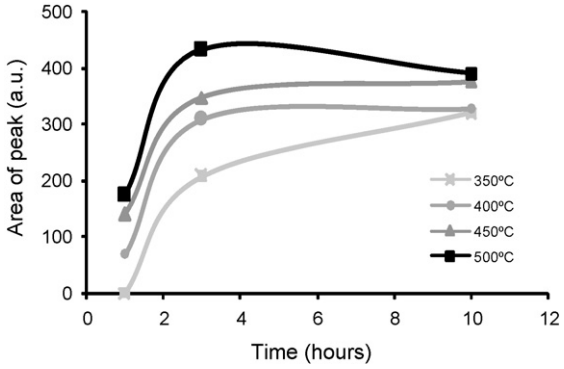

Fig. 3. Area of GXRD peaks on coatings fromTiO_2 sol B for different heat treatments.

3.3. Textural and morphological properties of TiO_2 thin films

Other relevant property related with photocatalytic activity is the specific surface area (S_s). Since no experimental techniques are available to measure this property in coatings an alternative procedure was used. Glass micro-spheres were coated with TiO_2 sols A and B with 3% of PEG and sintered at different temperatures and times. The specific surface area was measured by N_2 adsorption BET method and S_s of the coatings were calculated using Eq. (2). Fig. 5 shows the specific surface area of the TiO_2 coatings sintered for 3 h at different temperatures. At 350 °C low values of S_s are observed probably due to the incomplete removal of organic residues, still present in the structure. Above this temperature, S_s increases up to a maximum situated around 400–450 °C. For sol A this maximum (25 m^2/g) maintains quite constant

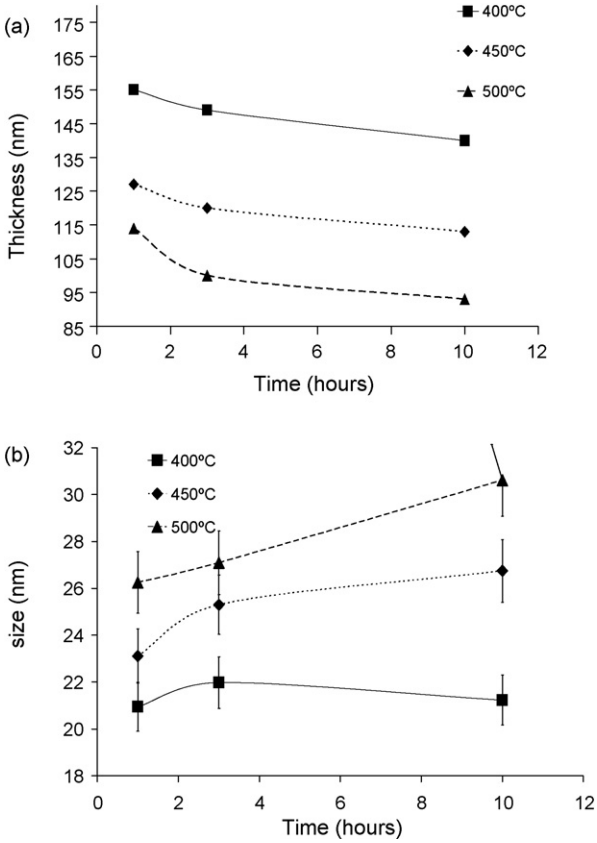

Fig. 4. Crystal size and thickness of coatings obtained from TiO_2-sol B for different treatments.

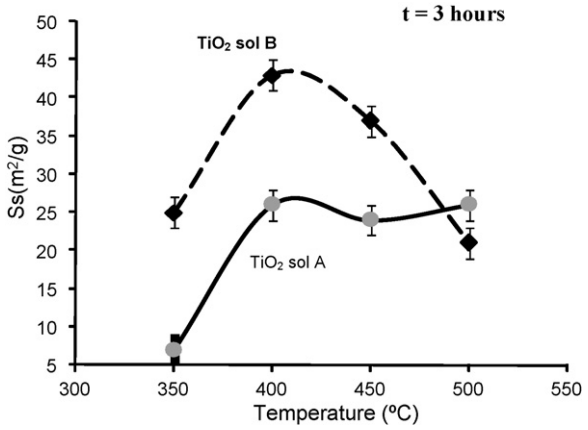

Fig. 5. Specific surface area (S_s) of TiO_2 coatings from sol A and B as a function of sintering temperature.

when temperature increases, indicating that maximum density has been reached around 400 °C. On the other hand, for TiO_2 sol B, the maximum specific surface area is near 43 m^2/g, suggesting coatings with more porous structure. When temperature increases S_s decreases and a gradual closing and collapse of the structure takes places, down to reach the S_s value of dense coatings from TiO_2-sol A. For these conditions (500 °C, 3 h), similar results for both preparation routes were obtained.

The evolution of S_s with sintering time (1, 3 and 10 h) was also studied observing a decrease likely associated with the partial collapse or densification of the coating structure.

FE-SEM was used to analyse the morphology (homogeneity and porosity) of the coated microspheres (Fig. 6). Micrograph 6(a) shows the total crystallisation of TiO_2 coating, with a narrow crystal size distribution centred around 27 nm, in good agreement with the values obtained by GXRD. Coatings produced by TiO_2-sol B show a more porous structure compared with TiO_2-sol A, micrographs Fig. 6(c) and (b), confirmed by S_s measurements.

3.4. Photocatalytic activity

The effect of sintering time in the photocatalytic activity was evaluated for TiO_2 thin films prepared using sol A and sol B routes treated at 500 °C. The TCE conversion curves for TiO_2 samples prepared with a 3% PEG treated during 1, 3 and 10 h are shown in Fig. 7. Photocatalytic curves present similar trends, decreasing the TCE conversion with the sintering time and gas flow. A 90% TCE conversion was obtained for 1 h sintering time and 50 mL min^{-1} gas flow. When catalysts prepared from sol A route were analysed similar results were obtained. As described in Fig. 5, the specific surface area of coatings prepared from both sols and treated at 500 °C/3 h was similar and thus, a comparable photoactivity is expected. Longer sintering times lead to a decrease in the photocatalytic activity independent of the sol type. This effect is especially relevant when sintering time increases from 3 to 10 h. According to previous data, TiO_2-anatase was the only phase detected, and crystal fraction and particle size do not significantly change with sintering time from 3 to 10 h. Thus, the reduction of photoactivity with sintering time should mainly be related to the densification of the coatings and the subsequent decrease of the surface area and porosity. Photoactivity data were collected in

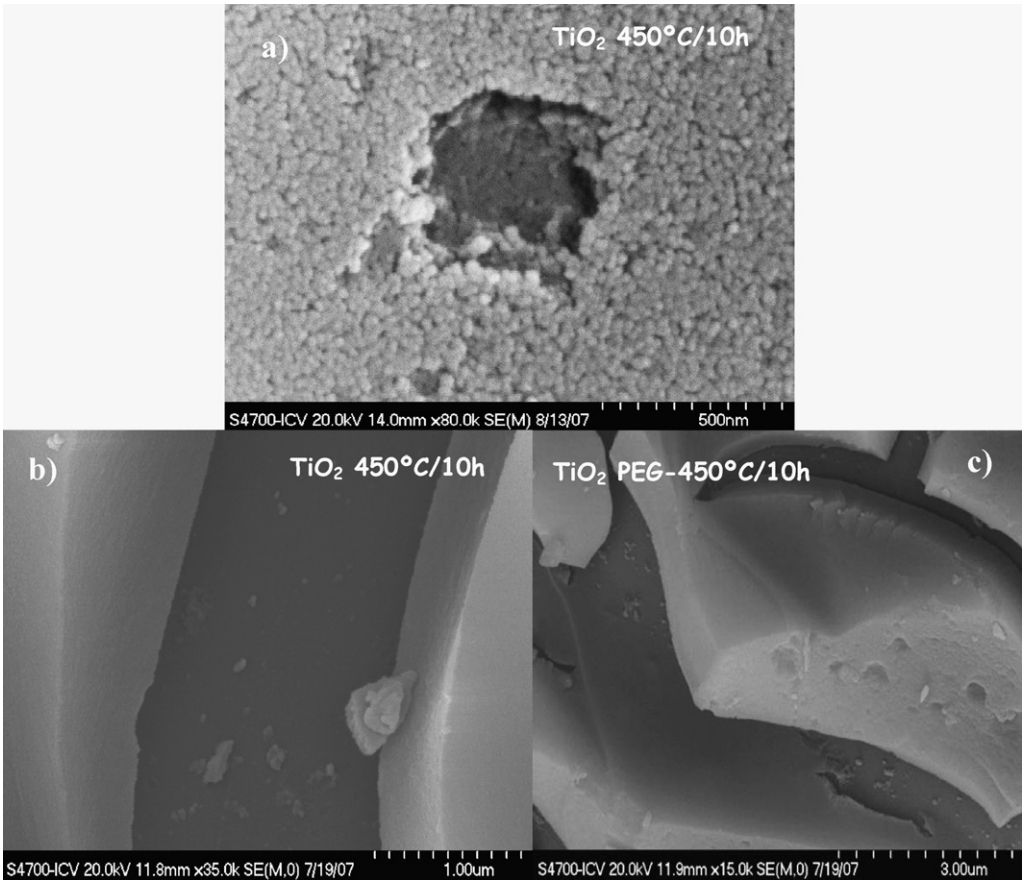

Fig. 6. FE-SEM microphotographs of microspheres coated and treated at 450 °C for 10 h from (a) and (b) TiO_2-sol A and (c) TiO_2-sol B.

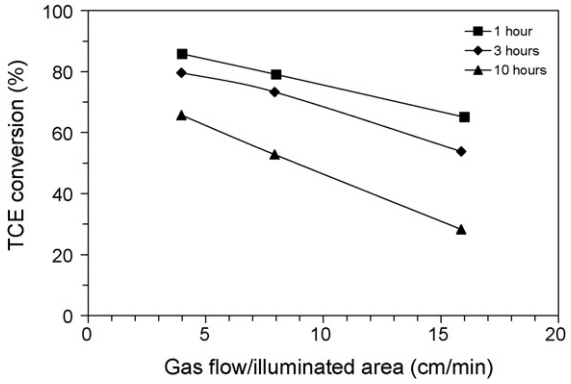

Fig. 7. Effect of the sintering time in the TCE conversion as a function of the total gas flow refereed to illuminated area for samples prepared from TiO_2-sol B treated at 500 °C.

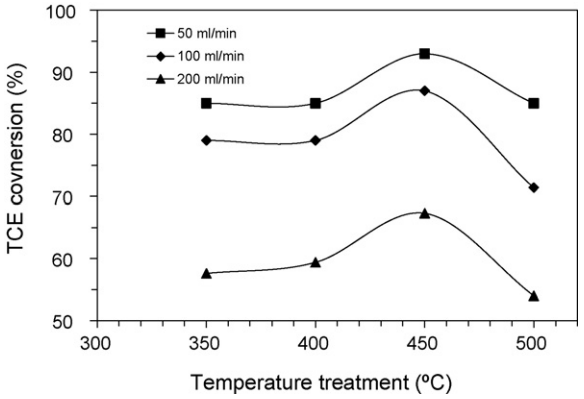

Fig. 9. Influence of the sintering temperature in the photocatalytic activity for two-layer coatings prepared by sol B with a 3% PEG for different total gas flow.

steady state conditions and deactivation of the catalyst was not observed.

The effect of the incorporation of PEG on the photocatalytic activity was also evaluated by comparing samples prepared from TiO_2-sol A and TiO_2-sol B treated at 450 °C during 3 h through the degradation of TCE. The results are shown in Fig. 8 varying the total gas flow from 50 to 200 ml min^{-1}. The plot clearly shows that the increase of porosity produced by the inclusion of PEG causes an augment of around 20% in the TCE conversion. The addition of PEG and its further elimination during the heat treatment lead to an increase of surface area and porosity of the samples reducing the internal mass transfer limitation of the pollutant to the active sites [45].

To make this behaviour more visible, we studied the influence of sintering temperature on the photoactivity of samples with 3% of PEG heat treated between 350 and 500 °C for 3 h (coating thickness around 180 nm). Fig. 9 shows the TCE conversion values as a function of the treatment temperature for three different gas flows. A maximum is observed at 450 °C, corresponding to a TCE conversion higher than 90% at 50 mL min^{-1}. Higher treatment temperatures reduce the photoactivity of the coatings. Deng et al. obtained similar results for the gas-phase photo-oxidation of hexane over nano-size TiO_2 catalysts [46]. Zhu et al. [47] also analysed the effect of calcination temperatures (300–600 °C) in the degradation of phenol. According to DRIFT, XPS and XRD results, the authors conclude that heat treatments between 300 and 600 °C improve the degradation of phenol, as a consequent of a progressive elimination of the surface organic residue along with further crystallisation in the TiO_2-anatase phase.

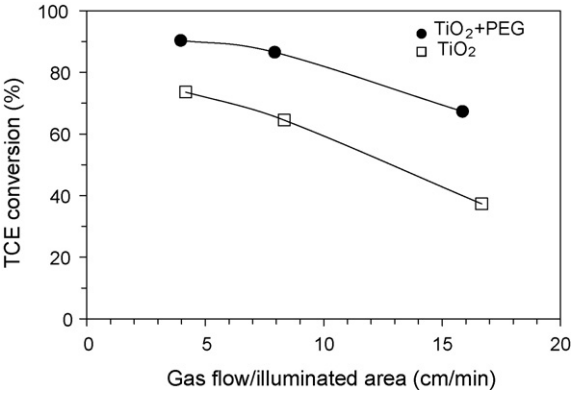

Fig. 8. Influence of the incorporation of PEG in the photocatalytic activity for samples treated at 450 °C during 3 h.

These results, mainly those of BET and GDXR analysis indicate that the photoactivity of titania coatings is closely related with the specific surface area. Although the presence of anatase is necessary, the crystal fraction and crystal size seem not to play a critical role in photocatalyst behaviour. These conditions implicate a compromise in temperature and times of sintering to ensure the appearance of TiO_2-anatase crystal phase, maintaining the high porosity of the layer.

4. Conclusions

Transparent, homogeneous and crack-free TiO_2-anatase nanocrystalline films were obtained through a simple and easy to scale-up sol–gel route incorporating PEG as pore generating agent.

The incorporation of PEG reduces the time necessary to obtain TiO_2-anatase to 3 h/350 °C. GDXR showed that crystal size augments with temperature and time of heat-treatment with typical crystal size below 30 nm. The crystalline fraction increases sharply with sintering time, indicating that crystallisation is complete after 3 h.

High porosity and surface area implicate higher contact surface exposed to TCE thus enhancing the degradation rate. The highest TCE conversion was obtained with samples sintered at 450 °C/1 h, the same conditions for obtaining the best compromise between the surface area and crystallinity. Further increase of sintering temperature causes a jumping down of the photocatalytic properties due to reduction of thickness and surface area related to densification of the coatings.

These results indicate that the photoactivity of titania coatings is closely related with the specific surface area. Although the presence of anatase is necessary, the crystal fraction and crystal size seem not to play a critical role in photocatalyst behaviour.

References

[1] http://www.epa.gov/iaq/voc.html
[2] EPA Act 1992 (Control of VOC Emissions from Petrol Storage & Distribution) Regulations (SI 374 of 1997), 1992.
[3] Council Directive 2004/42/CE OF THE EUROPEAN PARLIAMENT L of 21 April 2004 on the limitation of emissions of volatile organic compounds due to the use of organic solvents in certain paints and varnishes and vehicle refinishing products and amending Directive 1999/13/EC, 2004.
[4] M.A. Fox, M. Dulay, Chem. Rev. 83 (1995) 341.
[5] J.-M. Herrmann, Top. Catal. 34 (2005) 49.
[6] O. Carp, C.L. Huisman, A. Reller, Prog. Solid-State Chem. 32 (2004) 33.
[7] A.L. Linsebigler, G. Lu, J.T. Yates, J. Chem. Rev. 95 (1995) 735.
[8] R. Portela, B. Sánchez, J.M. Coronado, R. Candal, S. Suárez, Catal. Today 129 (1/2) 223.
[9] S. Suárez, J.M. Coronado, R. Portela, J.C. Martín, M. Yates, P. Avila, B. Sánchez, Environ. Sci. Technol. 42 (2008) 5892.

[10] G. Balasubramanian, D.D. Dionysiou, M.T. Suidan, V. Subramanian, I. Baudin, J.M. Laîné, J. Mater. Sci. 38 (4) (2003) 823.
[11] Y. Chen, D.D. Dionysiou, Appl. Catal. B 80 (2008) 147.
[12] Y. Chen, S. Lunsford, D.D. Dionysiou, Thin Solid Films 516 (2008) 7930.
[13] D. Mergel, D. Buschendorf, S. Eggert, R. Grammes, B. Samser, Thin Solid Films 371 (2000) 218.
[14] S. Yamanoto, T. Sumita, A. Miyashita, H. Naramoto, Thin Solid Film 401 (2001) 88.
[15] J. Lee, M. Kim, B. Kim, Water Res. 36 (2002) 1776.
[16] M.A. Fox, M.T. Dulay, Chem. Rev. 93 (1993) 341.
[17] K. Kato, A. Tsuzuki, H. Taoda, Y. Torii, T. Kato, Y. Butsugan, J. Mater. Sci. 29 (1994) 5911.
[18] H. Imai, H. Hirashima, J. Am. Ceram. Soc. 82 (1999) 2301.
[19] J.H. Schattka, D.G. Schukin, J. Jia, M. Antonietti, R.A. Caruso, Chem. Mater. 14 (2002) 5103.
[20] U. Cernigoj, U.L. Stangar, P. Trebse, U.O. Krasovec, S. Gross, Thin Solid Film 495 (2006) 327.
[21] S. Bu, Z. Jin, X. Liu, T. Yin, Z. Cheng, J. Mater. Sci. 41 (2006) 2067.
[22] H. Choi, E. Stathatos, d.D. Dionysios, Appl. Catal. B. 63 (2006) 60.
[23] J. Yu, X. Zhao, J. Du, W. Chen, J. Sol–Gel Sci. Technol. 17 (2000) 163.
[24] Y. Kotani, T. Matoda, A. Marsuda, T. Kogure, M. Tatsumisago, T. Minami, J. Mater. Chem. 11 (2001) 2045.
[25] J.H. Schattka, e.H.M. Wong, M. Antonietti, R.A. Caruso, J. Mater. Chem. 16 (2006) 1414.
[26] Y. Chen, E. Stathatos, D.D. Dionysiou, Surf. Coat. Technol. 202 (2008) 1994.
[27] S. Bu, Z. Jin, X. Liu, H. Du, Z. Cheng, J. Sol–Gel Technol. 30 (2004) 239.
[28] K. Kajihara, T. Yao, J. Sol–Gel Sci. Technol. 17 (2000) 173.
[29] K. Kajihara, K. Nakanishi, K. Tanaka, K.K. Hirao, N. Soga, J. Am. Ceram. Soc. 81 (1998) 2670.
[30] K. Kajihara, T. Yao, J. Sol–Gel Sci. Technol. 12 (1998) 193.
[31] A. Testino, I.R. Bellobono, V. Buscaglia, C. Canevali, M. D'Arienzo, S. Polizzi, R. Scotti, F. Morazzoni, J. Am. Chem. Soc. 129 (2007) 8566.
[32] H. Cheng, J. Ma, Z. Zhao, L. Qi, Chem. Mater. 7 (1995) 663.
[33] R.R. Bacsa, Kiwi, J. Appl. Catal. B 16 (1998) 19.
[34] T. Peng, D. Zhao, K. Dai, W. Shi, K. Hirao, J. Phys. Chem. B 109 (2005) 4947.
[35] D. Gumy, C. Morais, P. Bowen, C. Pulgarin, S. Giraldo, R. Hajdu, J. Appl. Catal. B 63 (2006) 76.
[36] H. Yin, Y. Wada, T. Kitamura, S. Kambe, S. Murasawa, H. Mori, T. Sakata, S. Yanagida, J. Mater. Chem. 11 (2001) 1694.
[37] M. Guglielmi, S. Zenezini, J. Non-Cryst. Solids 121 (1990) 303.
[38] J. Yu, X. Zhao, Mater. Res. Bull. 35 (2000) 1293.
[39] G.S. Herman, Y. Gao, T.T. Tran, Surf. Sci. 447 (2000) 201.
[40] M. Guglielmi, G. Brusatin, N. Tombolan, Riv. Staz. Sper. Vetro Sup. 23 (1993) 495.
[41] A. Durán, M.I. Nieto, Proceedings of XV International Congress on Glass 2a (1989) 5.
[42] J. Gallardo, P. Galliano, A. Durán, J. Sol–Gel Sci. Technol. 19 (2000) 393.
[43] Y. Djaoued, S. Badilescu, P.V. Ashrit, D. Bersani, P.P. Lottici, J. Sol–Gel Sci. Technol. 24 (2002) 247.
[44] Y. Li, T.J. White, S.H. Lim, J. Solid State Chem. 177 (2004) 1372.
[45] S. Suárez, M. Yates, P. Avila, J. Blanco Catal. Today 105 (2005) 499.
[46] X. Deng, Y. Yue, Z. Gao, Appl. Catal. B 39 (2002) 135.
[47] J. Zhu, J. Yang, Z.-F. Bian, J. Ren, Y.-M. Liu, Y. Cao, H.-X. Li, H.-Y. He, K.-N. Fan, Appl. Catal. B 76 (2007) 82.